Journal of Computational Statistics and Modeling, Vol. 1, No. 2, 125-138, December 2021

Mathematical Modeling of Behavior of Retrofitted RC Frames

Ali Moafi [1], Ali Kheyroddin[2], Hamid Saberi[3]*, Vahid Saberi[3]

[1] MSc, Structural Engineering, University of Eyvanekey, Semnan, Iran.

[2] Professor, Faculty of Civil Engineering, Semnan University, Semnan, Iran.

[3] Assistant Professor, Faculty of Civil Engineering, University of Eyvanekey, Semnan, Iran.

Recieved: 21/04/2021 Accepted: 04/11/2021

Abstract: Due to several reasons as the low resistance of constructed concrete and also change in codes or application of structures, some concrete frames need to be retrofitted. By adding the steel prop and curb to the reinforced concrete, many parameters such as ductility, resistance, and stiffness change. This study numerically investigates the impact of adding the prop and curb, slit damper, gusset plate, and also prop with a ductile ring on stiffness, resistance, energy dissipation, and ductility of RC frames. For this purpose, the effect of the aforementioned methods on the linear and nonlinear moment frame behavior of reinforced concrete under monotonic loads has been numerically investigated using the ABAQUS software. In the present study, 12 samples of reinforced frames with one story and one span were retrofitted by different methods. The novelty of the paper was using such props and slit damper in RC frames. The results obtained from the modeling showed that the retrofitted frame with a ring, slit dampers, and gusset plate also showed better behavior in terms of resistance and stiffness compared to the RC frame and the sample with slit damper and prop with a ductile ring as well as compared to the sample with the prop and curb showed more ductility and energy dissipation.

Keywords: RC moment resisting frame, Ductile ring, Slit damper, Steel prop, Gusset plate

Mathematics Subject Classification (2010): 97D70, 62H15.

*Corresponding Author: saberi.hamid@gmail.com

1. Introduction

In recent decades, numerous earthquakes have caused severe damage or have led to the collapse of old structures. Many existing reinforced concrete (RC) frame buildings were designed and constructed under the old seismic codes and regulations as those details are often not enough for proper seismic behavior, particularly in the beam–column connections, and or the lateral and horizontal displacement of them are not in safe range. Therefore, these deficient frames often do not resist earthquakes and need to be strengthened. For this purpose, different approaches have been proposed by researchers. In recent years, adding steel braces to concrete moment resisting frames (MRFs), jacketing with thin plain concrete or high performance fiber reinforced cementitious composites HPFRCC, flat and corrugated steel plate jacketing, attachment of steel plates, using of FRP composite material as externally bonded sheets, have used for local and general retrofitting of deficient RC frames. Each of the preceding methods can be used for upgrading and improving linear and nonlinear behavior of RC frames such as rigidity, ultimate strength, and ductility. Also, many researchers have investigated these mentioned methods for upgrading the behavior of the deficient RC beam-column connection experimentally and numerically.

Sharbatdar et al. (2012) used this idea with other schemes that were called "steel prop and curb". They retrofitted the damaged, weak exterior RC beam-column connection using this technique experimentally. The main idea of this technique was the use of the stiff members as steel props which acted as a resistant arm and the steel curbs for confining of the reinforced concrete beam and column. So this diagonal system decreases the forces and damages in the damaged panel zone consequently Sharbatdar et al. (2012). Emami et al. (2015) made numerical work on the abilities of the steel props and curbs method at strengthening of RC frame and investigated the global behavior of the strengthened frames by this method. Using the double-sided steel curb and prop system results in decreased shear stress in the panel zone and is followed by the limited crack formation in this area. On this basis, the formation of X shape cracks in the panel zone occurs in displacements higher than reference connections, determining that the system can be used for shear strengthening of panel zone in concrete structures Kheyroddin et al. (2016). Oh et al. et al. (2009) used slit dampers at steel beam-column joints for the first time in the literature. Performing four full scale beam-column joint experiments, the researchers managed to dissipate the energy of the applied cyclic loads without causing any damage to the columns and beams. They investigated the behavior of the steel dampers of different geometric shapes in IPE

type steel beams under cyclic loadings, different from other researchers. Shafaei et al. Shafaei et al. (2014) studied a practical seismic retrofit method named "joint enlargement using pre-stressed steel angles", based on a two-dimensional enlargement of non-seismically detailed external beam–column joints of existing RC structures using steel angles that were mounted using pre stressed cross-ties. There were other studies for retrofitting RC frames in recent years Andalib et al. (2014, 2019); Hemmati et al. (2020, 2018); Kheyroddin et al. (2019); Sepahrad et al. (2019).

As discussed, many studies have been conducted on retrofitting frames with steel elements to enhance the performance of these props, slit dampers, and gusset plates such as resistance increasing, ductility, and energy absorption. However, nothing has been done in applying the ductile ring at the center of the prop and retrofitted reinforce concrete beam-column joints using slit damper and gusset plate connection to the RC frame and comparing this sample with various states, so far. In this regard, thirteen numerical samples including the RC frame, the RC frame with props, the RC frame with the slit damper, the RC frame with the gusset plate, and the RC frame with the prop with ductile rings, have been studied.

2. Simulation and Verification

An experimental investigation has been conducted in order to validate the numerical method and gain a deeper understanding of the nature of the items of finite elements in the frame structure. The test models chosen for study were the large-scale, one-span, one-story plane frame Cranston and Cracknell (1969). The dimensions of the frame and details of the loading are shown in Fig. 1. The details of reinforcement layout for the frame are shown in Fig. 2. The concrete and the steel material properties are summarized in Table 1.

Table 1: Material properties used in the test frame Cranston and Cracknell (1969)

f'_c (MPa)	E_c (MPa)	f'_t (MPa)	ϵ_{cr}	ϵ^*_{cu}	V^*
18.9	18980	2.7	0.00014	0.007	0.17
f_y (MPa)	E_s (MPa)	E^*_s (MPa)	ϵ_{su}	ϵ_{sy}	$f_{y(stirrups)}$ (MPa)
440	200000	6200	0.15	0.0022	310

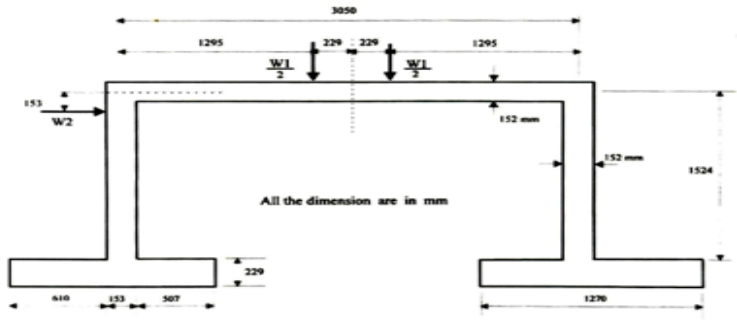

Figure 1: Details of test frame Cranston and Cracknell (1969)

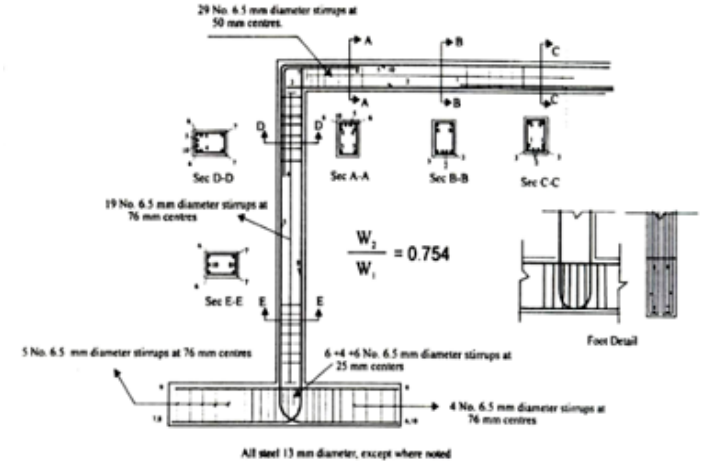

Figure 2: Reinforcement details of test frame Cranston and Cracknell (1969)

Two main concrete failure mechanisms are cracking under tension and crushing under compression. For simulations of concrete in ABAQUS, according to its brittle behavior, Concrete Damage Plasticity (CDP) model was used. The parameters describing the performance of concrete are determined for uniaxial stress. Table 2 shows the model's parameters characterizing its performance under compound stress.

Table 2: Suggested parameters of CDP model under compound stress

Viscosity parameter	*kc*	*Eccentricity* (ϵ)	Ψ	f_{b0}/f_{c0}
0.001	0.6667	0.1	30	16

For modeling of concrete 20-node solid element, C3D20R has been used, which is a cubic element with 20 nodes. Each node has 6 degrees of freedom, 3 translational and three rotational degrees of freedom. For modeling of reinforcements, Truss elements, T3D2 were used. Another material used and modeled in this study is steel. For the definition of plastic properties of steel, a bilinear stress-strain curve has been used. Defined material has kinematic hardening properties. Different mesh sizes were used for calibration of the frame, and ultimately, $50 \times 50\ mm^2$ mesh sizes were chosen (for concrete and reinforcement) because of the accuracy of results. Force-displacement diagrams of the experimental and finite element (numerical) models of ordinary RC frame are presented in Fig. 3. Observing the situation of the experimental and numerical frame at ultimate displacement, the location of cracks and plastic hinges can be investigated. As Figs. 4 shows, location of plastic hinges and Compressive and tensile damage in a numerical model can be observed, which have an excellent coincidence with results of the experimental model.

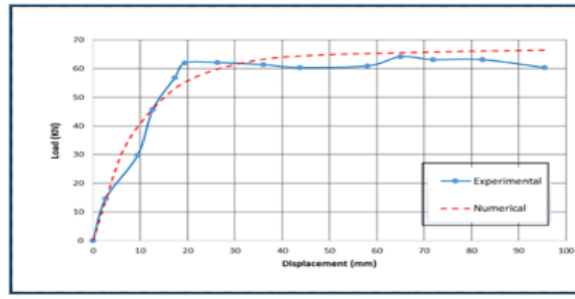

Figure 3: Verification of numerical FE model of ordinary RC frame

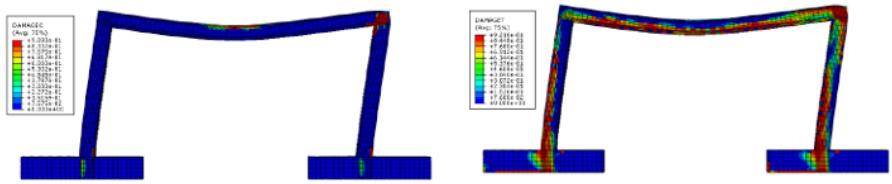

Figure 4: Compressive and tensile damages of ordinary frame

3. Modeling and Results

For investigating effects of prop and curb, slit damper, gusset plate, and also prop with a ductile ring and curbs on RC frames, twelve verified frames were modeled and strengthened at every side of beam-column connections and were then subjected to monotonic lateral loading at the top of the frames separately like the test frame. The ring should be ruptured along the weld line and not along its line or another line [according to the previous studies noted in the following (Eq. 1)] before the prop is buckled. Schematic retrofitting of specimens are presented in Fig. 5. Table 3 summarizes simulated models specifications. A mesh size in the finite element simulation is shown in Fig. 6.

$$2\mathrm{M}_p = \frac{P.R}{2} \rightarrow \frac{4M_p}{R}$$

$$\mathrm{M}_p = \frac{t^2 l \sigma_y}{4} \tag{3.1}$$

$$\mathrm{P} = \frac{t^2 l \sigma_y}{R}$$

The push diagram of samples is shown in Fig. 7. The loading-deflection curves of the reinforced frames show that stiffness, ultimate point, and energy dissipation are increased in all samples.

As you can see in terms of compressive damages inflicted on the frames, in the right-side panel zone, the upper part of the beam has been damaged, and in terms of tensile damage, the under part of the beam, and columns and even the foundations have been damaged. The extent of tensile and compressive damages of frames have been shown in Figs. 8 to 11.

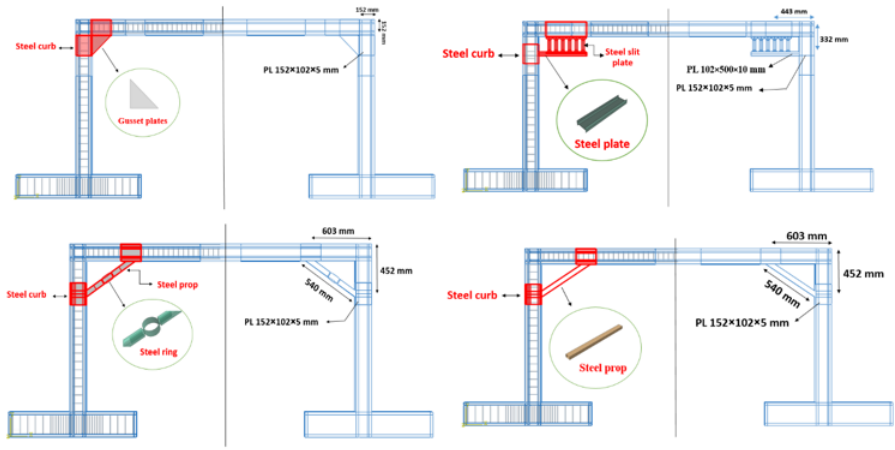

Figure 5: Proposed strengthening method of frame used in this study

Table 3: Mechanical properties of steel

	Steel prop and ring							
Specimen	ν	Curb(Box)(mm)	Outer diameter (mm)	Ring thickness (mm)	$prop(Box)(mm)$	$f_y(MPa)$	$f_u(MPa)$	$E_s(MPa)$
FR1			104	7	$50 \times 30 \times 7$			
FR2	0.25	$152 \times 102 \times 5$	104	10	$50 \times 30 \times 10$	240	400	2.1×10^5
FR3			104	14	$50 \times 30 \times 14$			

	Slit damper								
Specimen	ν	Curb(Box)(mm)	B (mm)	thickness (mm)	$H(mm)$	$r(mm)$	$Plate(mm)$	$f_y(MPa)$	$f_u(MPa)$	$E_s(MPa)$
FD1			30	3	100	20	$102 \times 500 \times 10$			
FD2	0.25	$152 \times 102 \times 5$	30	6	100	20	$102 \times 500 \times 10$	288	464	2.1×10^5
FD3			30	9	100	20	$102 \times 500 \times 10$			

	Steel prop and gusset plate					
Specimen	ν	Curb(Box)(mm)	gusset plate (mm)	prop (Box)(mm)	$f_y(MPa)$	$f_u(MPa)$	$E_s(MPa)$
FP1				$50 \times 30 \times 3$			
FP2				$50 \times 30 \times 4.5$			
FP3				$50 \times 30 \times 6$			
FS1	0.25	$152 \times 102 \times 5$	$200 \times 200 \times 3$		240	400	2.1×10^5
FS2			$200 \times 200 \times 6$				
FS3			$200 \times 200 \times 9$				

Figure 6: Mesh configurations for reinforcement frames

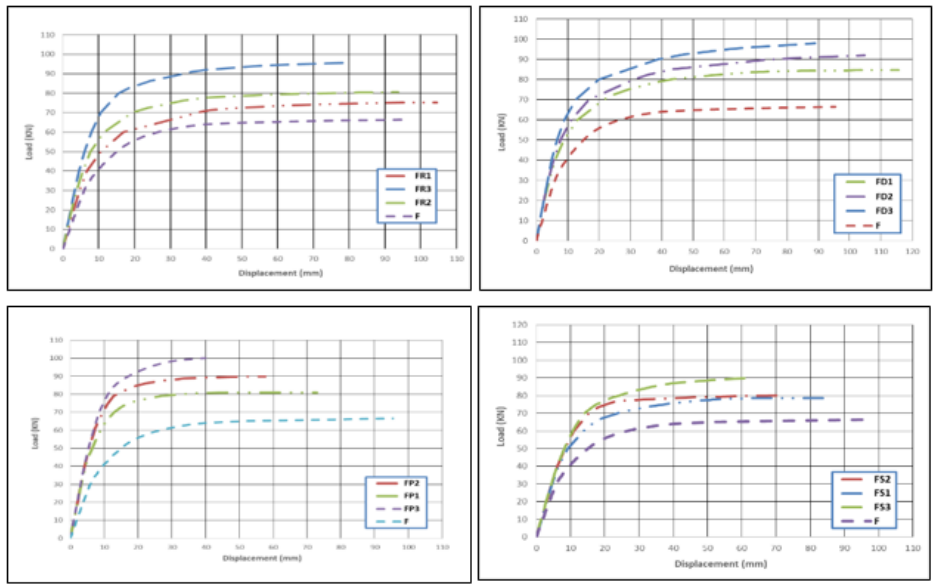

Figure 7: Load-deflection curves for frames reinforced

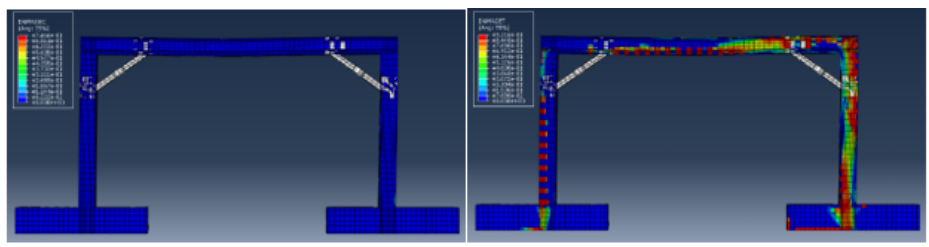

Figure 8: Compressive and tensile damages of FR3 frame

Location of cracks and tensile cracks pattern in strengthened frames are deduced that the proposed strengthening methods can relocate the tensile cracks

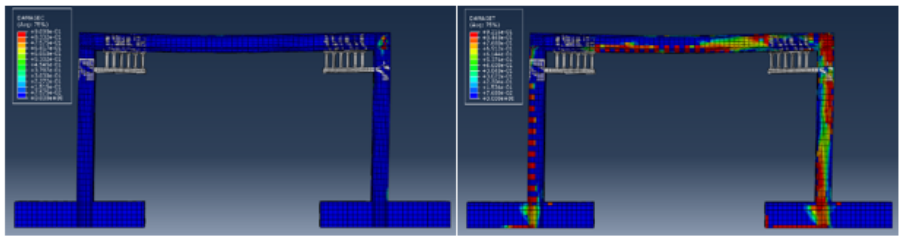

Figure 9: Compressive and tensile damages of FD3 frame

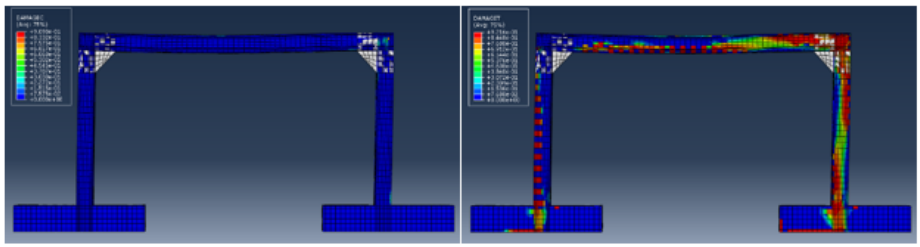

Figure 10: Compressive and tensile damages of FS3 frame

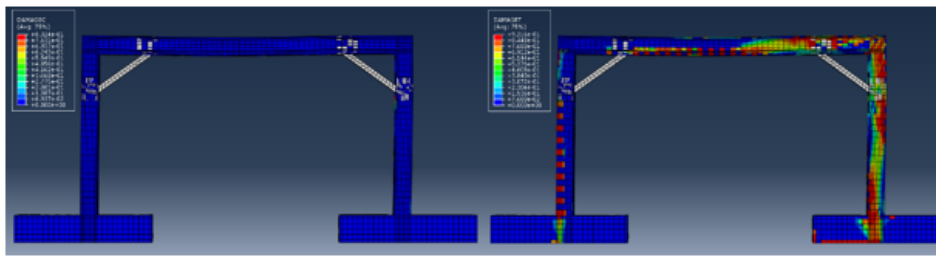

Figure 11: Compressive and tensile damages of FP3 frame

of the beam from the vicinity of beam column joint to away of steel curbs and therefore the plastic hinges are formed far from beam-column joints. In Figs. 8 to 11, the tensile damages inflicted on the frame in the beams and foundation parts have been decreased; in addition, vertical displacement and tensile damages of the beam have remarkably decreased.

Fig. 12 shows the yielding of reinforcement elements, showing how they deform under loading. Ductility is one of the most important parameters for the seismic evaluation of a structure. To obtain the ductility, using the push diagram for determining the force and the yield displacement is accompanied by some difficulties.

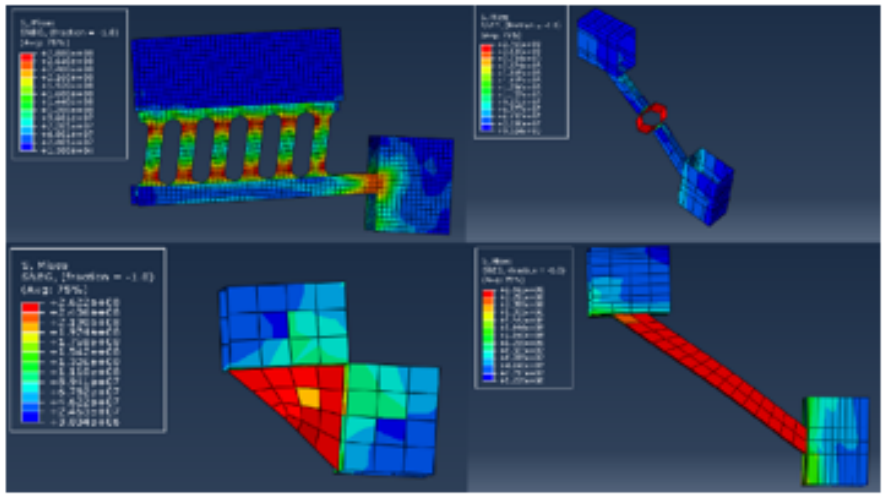

Figure 12: Yielding of reinforcement elements in FD2, FR2, FS2, and FP2

This difficulty is due to the fact that the push diagram does not have a certain yield point. The yield point in the push diagram is not clear, and it is due to several factors, including the non-linear behavior of the material and starting the yield in different parts of the structure at different levels due to the indeterminacy of the structure and re-distribution of forces Maheri et al. (2003). The results obtained from the bilinear diagram of the test frames are listed in Table 4. In the above table, $\mu = \frac{\Delta u}{\Delta' y}$. For reinforced frames, $\Delta' y$ stands for the displacement point at which the reinforcements start yielding. As you can see, as the reinforcement elements are added, although the ultimate displacement decreases, however, the ductility coefficient increases. For each sample, the lateral stiffness (K) level is calculated in each drift. The calculation trend of stiffness is by dividing the maximum force of each monotonic by its corresponding displacement and is consecutively calculated for each drift. The lateral stiffness is shown in Table 4. Results of inspections have shown that the proposed elements have a desirable ductility while showing a high capacity for energy dissipation. In addition, the results of these investigations show that energy absorption and ductility are more suitable under a circular ring geometry while it also works as a fuse in the responsibility of controlling the prop's buckling and providing the required ductility. Table 4 shows the values of stiffness, ductility, and energy dissipation (E).

Table 4: Specification of yield point, ultimate point, ductility, stiffness and energy dissipation

Specimen	$K(\frac{n}{mm})$	Yield		Ultimate		μ	$E(kj)$	$\frac{K}{K(F)}$	$\frac{PU}{PU(F)}$	$\frac{\mu}{\mu(F)}$	$\frac{E}{E(F)}$
		$\Delta_y(mm)$	$P_y(KN)$	$\Delta u(mm)$	$Pu(KN)$						
F	2475	20	60	95.37	66	4.75	12.7	1	1	1	1
FR1	3071	18.4	66	109.5	76	5.95	17.4	1.24	1.15	1.25	1.37
FR2	3940	16.27	72	93.6	81	5.75	17.6	1.59	1.22	1.21	1.38
FR3	5044	13	83	71.62	96	5.51	17.4	2.03	1.45	1.16	1.37
FD1	3395	18.66	72.5	115.5	84.4	6.19	21	1.37	1.28	1.30	1.65
FD2	3451	20	80	104.8	92	5.24	20.5	1.39	1.39	1.1	1.61
FD3	4234	17.33	90	88.88	97.8	5.12	18.5	1.71	1.48	1.07	1.45
FS1	3230	18.26	67.3	100	78.6	5.47	16.3	1.30	1.19	1.15	1.28
FS2	4090	17.88	74	86	80.4	4.81	15.3	1.65	1.22	1.01	1.20
FS3	4217	14.22	80	62.48	90	4.39	11	1.70	1.36	0.92	0.86
FP1	5060	12.36	74	72.97	81	5.9	15.3	2.04	1.23	1.24	1.20
FP2	5802	11.6	78	57.65	89.7	4.96	14.5	2.34	1.36	1.04	1.14
FP3	6251	11.5	87	40	100	3.48	7	2.52	1.51	0.73	0.55

4. Conclusions

In the FP1, FP2, and FP3 samples in which the RC frame was retrofitted using the steel prop and curb, the frame capacity was increased about 1.51 times which brought a satisfactory result for increasing the capacity. The destruction trend of these samples is that the prop under the compressive force buckled out-of-plane, and subsequently, the tensile prop was ruptured. By continuing the loading after removing the steel prop from the system, shear cracks were formed in columns and caused to rupture of the RC frame. To increase the strength and the lateral stiffness of the structure, using a steel prop is an effective method.

However, they are not efficient enough to obtain ductility. However, on the contrary, by using ductile rings without gaps in prop (FR1, FR2, and FR3), the ductility can increase. The results show that props remained intact, and only rings were ruptured. In other words, rings were acted as fuses that are simply replaceable.

Using the slit damper and curb at concrete beam-column joints in RC structures is a suitable method, and it is believed that the energy absorption is concentrated only at the slit dampers rather than at the beams, and the plastic deformation was concentrated at the slit dampers while the beams and columns remained almost elastic. The results also show that the use of slit dampers increases capacity and ductility.

This proposed strengthening method (FS1, FS2, and FS3) increased remarkably the strength, stiffness, and ductility factor of frames but by adding gusset plate's thickness decreased the ductility factor relatively. This proposed system could severely decrease the maximum plastic strain tensile of concrete adjacent to the joint and relocate the damages and plastic hinges to the vicinity of the steel curb.

References

Andalib, Z., Kafi, M.A., Kheyroddin and A., Bazzaz, M. (2014), Experimental investigation of the ductility and performance of steel rings constructed from plates. *J Constr Steel Res*, **103**, 77-88.

Andalib, Z., Kafi, M.A., Kheyroddin, A., Bazzaz, M., and Momenzadeh, S.B. (2019), Numerical evaluation of ductility and energy absorption of steel rings constructed from plates. *Engineering Structures*, **169(15)**, 94-106.

Cranston, W. B. and Cracknell, J. A. (1969), *Tests on reinforced concrete frames*

2: portal frames with fixed feet. Cement and Concrete Association, London, TRA/420.

Hemmati, A., Kheyroddin, A. and Farzad, M. (2020), Experimental study of reinforced concrete frame Rehabilitated by concentric and eccentric bracing., **8(1)**, 97-108.

Hemmati, S.A., Bafghi, M.A.B. and Kheyroddin, A. (2018), Experimental investigation of pod on the behavior of all-steel buckling restrained braces. *Journal of Constructional Steel Research*, **150**,186-194.

Kheyroddin, A., Khalili, A., Emami, E. and Sharbatdar, M.K. (2016), An innovative experimental method to upgrade performance of external weak RC joints using fused steel prop plus sheets. *Steel Compos Struct* , **21(2)**, 443-460.

Kheyroddin, A., Gholhaki, M. and Pachideh, G.H. (2019), Seismic evaluation of reinforced concrete moment frames retrofitted with steel braces using IDA and Pushover methods in the near-fault field. *Journal of Rehabilitation in Civil Engineering*, **7(1)**, 227-241.

Maheri, M.R., Kousari, R. and Razazan, M. (2003), Pushover test on steel X-brace and knee- braced RC frame. *Eng. Struct*, **25(13)**,1697-1705.

Oh, S.H., Kim, Y.J. and Ryu, H.S. (2009), Seismic Performance of Steel Structures with Slit Dampers. *Engineering Structures* , **31(9)**,1997-2008.

Sepahrad, R., Kheyroddin, A., Saljoughian, M. and Kafi, M.A. (2019), Experimental evaluation of RC frames retrofitted by steel jacket, X brace and X brace having ductile ring as a structural fuse, *Journal of Building Pathology and Rehabilitation*, **4**, 11.

Shafaei, J., Hosseini, A. and Marefat, M.S. (2014), Seismic retrofit of external RC beam–column joints by joint enlargement using prestressed steel angles. *Engineering Structures*, **81**, 265-288.

Sharbatdar, M.K., Kheyroddin, A. and Emami, E. (2012), Cyclic performance of retrofitted reinforce concrete beam-column joints using steel prop. *Constr Build Mater*, **36**, 287-294.